Pre- and postrestoration assessment of stream water–groundwater interactions: effects on hydrological and chemical heterogeneity in the hyporheic zone

Margaret A. Zimmer[1,2] and Laura K. Lautz[1,3]

[1]Department of Earth Sciences, Syracuse University, Syracuse, New York 13244 USA

Abstract: Reach-scale stream restoration with natural channel design is often used to improve stream ecosystem structure and function. Some investigators have studied the effects of restoration on the hyporheic zone, but most used space-for-time substitution instead of comparing the same reach before and after restoration. We examined spatial patterns of hyporheic exchange rates and geochemistry during base flow in a 30-m pool–riffle–pool sequence before and 1 y after the stream was restored by installation of a cross-vane and engineered rock-riffle. Prerestoration vertical hyporheic exchange rates were relatively uniform across the riffle bedform. Average downwelling was 30 cm/d at or upstream of the riffle, and average upwelling was 30 cm/d downstream of the riffle. Downwelling hyporheic exchange rates increased up to an order of magnitude adjacent to the cross-vane and in the engineered rock-riffle. Prerestoration porewater [NO_3^-] was distributed along a wide and continuous gradient (0.1–3.8 mg/L), with higher concentrations in areas of downwelling and lower concentrations in areas of upwelling. Postrestoration [NO_3^-] was distributed bimodally with relatively high concentrations (>1.6 mg/L) adjacent to the cross-vane and low concentrations (<1 mg/L) elsewhere. These results suggest that rapid flushing of surface water through the subsurface creates residence times too short to yield net changes in [NO_3^-] along flow paths around the cross-vane. Distinct zones of groundwater upwelling were present before and after restoration, but the size of the zone of upwelling increased downstream of the cross-vane after restoration, possibly because higher permeability material was placed over the original, lower permeability sediment during restoration, creating an effective anisotropy that favored horizontal flow and produced larger apparent zones of groundwater discharge.

Key words: surface-water-groundwater interactions, restoration, biogeochemistry, stream bed, Natural Channel Design, cross-vane, engineered rock-riffle

The movement of surface water and ground water into and out of the stream bed (hyporheic exchange) produces a unique streambed ecotone, referred to as the hyporheic zone. This zone can provide a spectrum of subsurface habitats that vary in availability of O_2 and nutrients, water temperature, and light intensity, depending on the spatial distribution of upwelling ground water and downwelling surface water (Gibert et al. 1990). Physical variables, such as bedform morphology, channel meandering, and hydraulic gradients beneath and adjacent to the stream, control a variable distribution of surface water and ground water in the hyporheic zone (Boano et al. 2006, Kasahara and Hill 2006, Hester and Doyle 2008). Furthermore, aquifer hydraulic conductivity can impede or enhance the movement of water across the stream–streambed interface (Morrice et al. 1998). This variability in water sources and environments influences the distribution of invertebrates and microbes that dwell in the hyporheic zone (Vervier et al. 1992, Marmonier et al. 1993, Hayashi and Rosenberry 2002, Boulton 2007). Streambed invertebrates and microbes affect streambed porosity (Edler and Dodds 1992), rates of metabolism and biogeochemical cycling in the stream and stream bed (Triska et al. 1993, Hendricks 1996, Hakenkamp et al. 2002, Battin et al. 2003, Lautz and Fanelli 2008), organic matter and pollutant breakdown (Smith and Lake 1993, Haack and Bekins 2000, Gandy et al. 2007), and the movement of material within and through the hyporheic zone (Stanford and Ward 1993,

E-mail addresses: [2]Present address: Division of Earth and Ocean Sciences, Duke University, Durham, North Carolina 27708 USA, margaret.zimmer@duke.edu; [3]lklautz@syracuse.edu

DOI: 10.1086/679514. Received 22 April 2013; Accepted 27 May 2014; Published online 2 December 2014 .
Freshwater Science. 2015. 34(1):287–300.

Strayer 1994). Thus, the natural heterogeneity of stream–streambed connectivity within the subsurface is important for maintaining ecosystem function (Gibert et al. 1994, Hancock et al. 2005).

The health of stream ecosystems can be negatively affected by anthropogenic activities, via pollution, alteration of exchange processes, and reduction of streambed permeability by siltation (Schälchli 1992, Brunke 1999, Brunke and Gosner 1997, Hancock 2002, Nogaro et al. 2010). Heterogeneities in streambed topography and streambed roughness increase hyporheic exchange (Stonedahl et al. 2012, 2013), but degradation of streambed reaches by sedimentation or erosion from upstream construction or increased runoff can homogenize streambed topography and limit exchange rates. Homogenization reduces the ability of the hyporheic zone to provide a unique environment for countless species of subsurface fauna. In the absence of a strong stream connection, diminished availability of dissolved O_2 (DO), light, and nutrients will limit productivity of the stream bed and reduce the diversity of invertebrates, which are important indicators of overall stream ecosystem health. In response, researchers have recommended restoration approaches that increase the vertical connectivity between streams and ground water (e.g., Boulton 2007, Kasahara et al. 2009, Hester and Gooseff 2010, 2011).

The USA spends billions of dollars each year on stream restoration (Bernhardt et al. 2005) to improve ecological, physical, and chemical conditions in degraded streams (Lave 2009). Most restoration projects are small scale (<1-km stream length) and are used to improve aquatic habitat, reduce sediment erosion through bank stabilization, and improve surface-water quality (Bernhardt et al. 2005). Many of these projects include channel remeandering, cross-vane installation, and bank armoring. Natural Channel Design (NCD), also known as the Rosgen method (Rosgen 1994) or river-classification approach (Hey 2006), is a tool used commonly in river restoration. However, the outcomes of <10% of completed restoration projects are assessed (Bernhardt et al. 2005), and hyporheic exchange is rarely included as a goal in restoration projects (Hester and Gooseff 2011). Therefore, little is known about the effectiveness of NCD restoration on stream structure, function, and hyporheic exchange.

Our study was focused on the effects of 2 techniques frequently used in NCD, cross-vane and engineered rock-riffle installation. Cross-vanes are large boulder dams typically installed at the heads of riffles or in glides to reduce bank erosion, establish grade control, improve ecological habitat, and focus stream energy to the thalweg (Rosgen 2001). Cross-vanes create a head differential from upstream to downstream of the cross-vane and focus flow to the channel center, so they typically deepen an excavated plunge pool immediately downstream of the structure (e.g., Daniluk et al. 2013). However, when cross-vanes are paired with engineered rock-riffles, the plunge pool is filled with boulders and cobbles, which increase turbulence and simulate a high-gradient riffle (Hester and Gooseff 2011).

Restoration features that enhance hyporheic exchange do so by enhancing the physical flow of water through the stream bed (Crispell and Endreny 2009, Hester and Gooseff 2011). A primary driver of hyporheic exchange is the local variation in head gradients between the stream and ground water, from such bedform topography as pool–riffle and step–pool sequences (Harvey and Bencala 1993, Kasahara and Hill 2006). Studies on streambed geochemistry and vertical hyporheic exchange rates around restoration cross-vanes showed that the hydraulic step across the structures produces high rates of downwelling immediately upstream of these structures (Lautz and Fanelli 2008, Crispell and Endreny 2009, Daniluk et al. 2013, Gordon et al. 2013), thereby creating hotspots of hyporheic exchange. Moreover, heterogeneity in sediment texture, morphology, and turbulence, as seen across rock-riffles, also affects hyporheic flow (Elliott and Brooks 1997, Cardenas et al. 2004, Cardenas and Wilson 2007, Ward et al. 2011). Investigators have examined the interactions between hyporheic exchange and groundwater discharge in heterogeneous stream beds (Marion et al. 2008, Sawyer and Cardenas 2009), but whether construction of restoration structures alters the interactions between hyporheic exchange and groundwater discharge by altering streambed sediment permeability is not known. Most research examining the effects of restoration on the hyporheic zone has been focused on identifying generalizable and predictable spatial patterns in hyporheic exchange or streambed geochemistry around restoration structures (Kasahara and Hill 2006, Lautz and Fanelli 2008, Crispell and Endreny 2009, Gordon et al. 2013).

NCD restoration designs often are based on natural features found at stable reference reaches (Rosgen 1998, 2011). Reference reaches are intended to represent predisturbance conditions for the specific stream degradation that the restoration is aiming to address (Rosgen 2011). Some investigators have compared hydrology and geochemistry of the hyporheic zone between restored and reference stream reaches representing the predisturbance condition (Becker et al. 2013, Daniluk et al. 2013), unrestored reaches representing the prerestoration degraded condition (Knust and Warwick 2009, Becker et al. 2013), or the same restoration site over time (Toran et al. 2012). However, we are unaware of any studies examining changes in hyporheic zone dynamics pre- and postrestoration at a single site. We addressed this gap in knowledge by measuring hyporheic zone exchange rates and geochemistry across the same stream reach before and 1 y after stream restoration.

METHODS

Site description

The study site was a 30-m pool–riffle–pool sequence in Chittenango Creek (Fig. 1A, B), an ungauged tributary to Oneida Lake, near Syracuse, New York, USA (lat 43°00′32.27″N, long 75°50′49.85″W, 178 m asl), with a 750-km^2 drainage area. Stream width averaged 12 m along the study reach. The site was restored in September 2011 by installation of a cross-vane across the head of the riffle and an engineered rock-riffle immediately downstream. The remaining portion of the stream bed is composed of coarse sand and gravel, the same material that was present prior to restoration. Discharge in the study reach (estimated from measurements of stream flow with an acoustic Doppler velocimeter) was 0.80 m^3/s at the time of the prerestoration assessment (August 2011) and 0.51 m^3/s at the time of the postrestoration assessment (August 2012).

Stream instrumentation and sampling

We surveyed the morphology of the study site with a Nivo 5.M total station (Nikon-Trimble Co., Tokyo, Japan), which has a spatial resolution <1 cm. Before restoration, we collected spatial information at 167 survey points to characterize positions of installed sampling equipment, bedform morphology, and water edge during baseflow conditions (Fig. 1A). After restoration, we collected spatial information at 219 survey points to recharacterize the position of installed sampling equipment and restoration structure, bedform morphology, and water edge during baseflow conditions (Fig. 1B). We surveyed more points after than before restoration to ensure accurate characterization of the complex topography around the restoration structure, including accurate representation of the break in slope between the cross-vane and rock-riffle. We imported survey points into ArcGIS and generated topography by interpolating between points with a spline algorithm.

We installed temperature profile rods (14 before and 10 after restoration) throughout the study reach to enable us to calculate vertical exchange rates in the stream bed (Fig. 1A, B). Fewer temperature profile rods were installed after than before restoration because of logistical constraints during the field season. Temperature profile rods contained 7 vertically stacked temperature sensors (iButton DS1922L, Maxim Integrated, San Jose, California). Six sensors were in the stream bed at 5-cm intervals to a depth of 30 cm, and 1 was in the water column (depth = 0 cm). The sensors recorded temperature at 10-min intervals throughout the summer field season before restoration and at 30-min intervals throughout the summer field season after restoration. We measured temperature at a coarser interval after restoration because of a longer deployment period and data storage limitations. We analyzed data collected over 7 continuous days during a representative baseflow period (i.e., no rain fell during this period) in each season.

For each sampling location, we calculated vertical water flux rates based on 1-dimensional heat transport modeling (Hatch et al. 2006, Gordon et al. 2012). This modeling method does not measure horizontal flow components, and in-stream bedforms can induce highly curvilinear hyporheic flow paths. Nevertheless, this method was valid for our purpose because the predominantly vertical exchange at the stream–streambed interface was the focus of our study. We used VFLUX (Gordon et al. 2012), a MATLAB 7.13 (R2011b) (The MathWorks, Inc., Natick, Massachusetts) program, to derive vertical flux rates at 2-h intervals during the 7-d baseflow period from the difference in amplitude of the propagated diurnal tem-

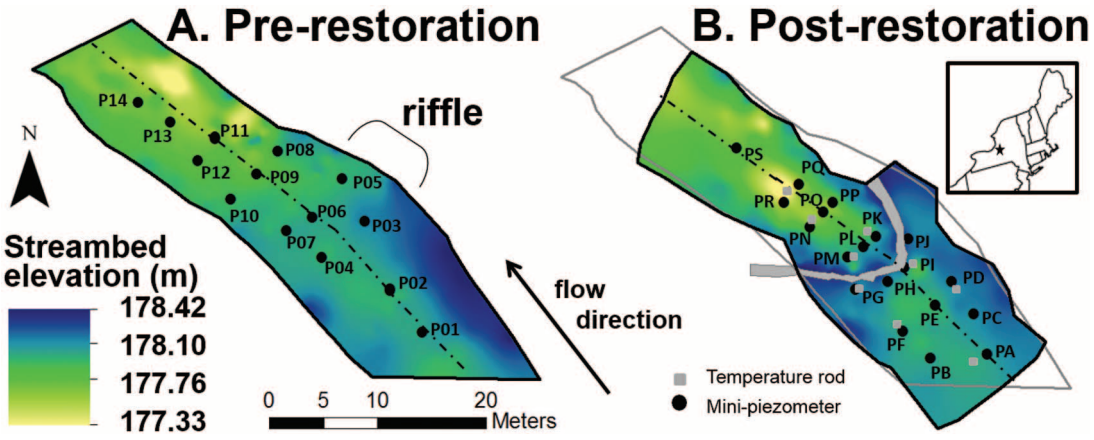

Figure 1. Map of study reach pre- and postrestoration, with location indicated by star in inset map of New York. A.—Prerestoration elevation and sites with co-located mini-piezometers and temperature profile rods. B.—Postrestoration elevation and sites with mini-piezometers or temperature profile rods. The aerial extent of the prerestoration site is shown as a grey outline on the postrestoration map. Longitudinal black dashed line represents cross-section of streambed elevations used to make Fig. 2.

perature signal measured at multiple depths (Hatch et al. 2006). Flux rates were calculated every 2.5 cm from a depth of 2.5 to 27.5 cm using sensor pairs spaced 5 and 10 cm apart (i.e., sensor spacing of 1 and 2 sensors). We created profiles showing change in vertical flux rates with depth by averaging the 2-h flux rates over the 7-d observation period to derive a single flux rate for each vertical observation point. To facilitate spatial comparison of vertical flux rates in plan view between pre- and postrestoration conditions, we averaged shallow flux rates at depths of 2.5 and 5.0 cm to derive one flux rate at the streambed interface. We averaged the 2 shallowest flux rates because most of the variance in vertical flux rates was observed in the upper 5 cm of the stream bed, and these shallow depths are most representative of the vertical exchange across the streambed interface.

Before restoration, we installed mini-piezometers at the 14 locations with temperature profile rods (Fig. 1A). After restoration, we installed mini-piezometers at 19 locations distributed around the 10 temperature profile rods (Fig. 1B). Mini-piezometers were constructed of polyvinyl chloride (PVC) pipe (1.27-cm inner diameter) with a 5-cm screen created by drilling a series of 0.3-cm-diameter holes in the pipe. We installed the mini-piezometers 17.5 cm below the stream–streambed interface, such that the 5-cm screen was centered at 15 cm depth. We used plastic tubing and a syringe to purge and sample pore water from the mini-piezometers. Each mini-piezometer was purged once prior to sample extraction.

We extracted all samples within a single 2-h period and filtered them through a 0.7-μM glass microfiber filter <8 h after sampling. We measured dissolved O_2 [DO], temperature, specific conductance (SC), and pH in the field. We measured dissolved anions (F^-, Cl^-, NO_3^-, SO_4^{2-}) and cations (Ca^{2+}, Na^+, Mg^{2+}, K^+) on a Dionex ICS-2000 ion chromatograph (Dionex, Sunnyvale, California). We measured NH_4^+, Br^-, and PO_4^{3-} but did not use them in the analysis because most values were below detection limits. We calculated [HCO_3^-] as the difference between total concentrations of anions and cations. We measured DO concentration in the field and calculated % saturation (Benson and Krause 1980, 1984) based on the average, minimum, and maximum stream and porewater temperatures (Table 1) and a barometric pressure of 757 mm Hg (the average of the minimum and maximum reported pressures for August 2011; National Oceanic Atmospheric Administration www.ncdc.noaa.gov/cdo-web/). We used barometric pressure data for August 2011 for pre- and postrestoration calculations because the maximum pressure for August 2012 was not available.

Rhodamine WT (RWT) is a fluorescent dye often used as a hydrologic tracer (Kilpatrick and Cobb 1985). While monitoring postrestoration conditions, we used a 24-h constant-rate injection of RWT at a site ~350 m upstream of the study site to observe tracer dilution in pore water at 15 cm depth during base flow. We calculated the % surface water in the pore water at each mini-piezometer at the end of the 24-h injection. The average plateau concentration of RWT during the injection period was 11.2 μg/L in the surface water measured near mini-piezometer PS (Fig. 1B). After plateau was reached, we sampled surface water near PS and pore water at each mini-piezometer every 30 min for the first 2 h and then every 2 h for the remainder of the experiment (n = 10 sampling periods). During the last sampling period, we also collected surface water at each mini-piezometer location. This snapshot of RWT in surface water at each mini-piezometer location showed somewhat variable mixing of RWT across the stream reach during plateau. RWT concentrations ranged from 7.93 to 10.17 μg/L. The last snapshot sample survey had systematically lower RWT concentrations than the plateau average of 11.2 μg/L because of dilution from a discharge increase from an upstream outflow. We assumed the range of RWT concentrations across the stream reach was constant through time and, therefore, that the range of observed RWT concentrations in the stream during the last sampling period (–0.76 to +1.47 μg/L from measurement at PS) was representative of the range of RWT concentrations during other times during the plateau. We used the assumed range of RWT concentrations in the water column across the study reach to estimate the possible range of % surface water in the pore water at each mini-piezometer.

We decanted the water samples in the field to minimize suspended sediment. We measured RWT in each sample at room temperature with an in-laboratory GGUN-FL30 fluorometer (Albillia Co., Neuchâtel, Switzerland). For quality control, we measured RWT concentrations in each sample twice, corrected for temperature during measurement, and used the sample average. To calculate % surface water in the pore water at each mini-piezometer location, we calculated the % difference between RWT concentrations in the pore water and in the surface water at each time step. We averaged the % surface water from the 7th, 8th, and 9th sampling periods to get a single % surface water value for each mini-piezometer location. We chose the later sampling periods to ensure that enough time had passed for the RWT concentrations to be at or near plateau in the porewater samples. The experiment lasted only 24 h, so it is possible that not all hyporheic flowpaths were equilibrated with RWT by the end of the study. Thus, % surface-water calculations are conservative.

RESULTS

Streambed morphology pre- and postrestoration

Pre- and postrestoration longitudinal streambed elevations differed markedly (Fig. 2). The reach average elevation

Table 1. Mean (range) solute concentrations in surface water and in surface-water (SW)-like and groundwater (GW)-like pore water pre- and postrestoration. Mean (range) of dissolved O_2 (DO) as % saturation (sat) was calculated from DO concentration and temperature for stream and porewater sites. Surface water temperatures were calculated from temperature profile rods at 0 cm depth (in stream column) averaged over 2-h sampling period at all profile locations. Porewater temperatures were calculated from temperature profile rods at 15 cm streambed depth averaged over 2-h sampling period at all profile locations. Bold indicates variables that differed significantly ($p < 0.01$) between SW-like and GW-like sites. – indicates no temperature or calculated DO % saturation postrestoration because temperature profile rods were not coincident with porewater sampling locations.

	Prerestoration				Postrestoration			
Solute	SW	Pore water	SW-like (P03, P04, P06, P07, P08, P10, P11, P12, P13, P14)	GW-like (P01, P02, P05, P09)	SW	Pore water	SW-like (PB, PF, PG, PH, PI, PJ, PK, PL, PM, PQ, PR, PS)	GW-like (PA, PC, PD, PE, PN, PO, PP)
Ca^{2+} (mg/L)	77.5	144.2 (78.5–395.3)	**84.3 (78.5–90.4)**	**239.9 (136.2–395.3)**	89.4	170.0 (85.2–371.8)	**89.5 (85.2–98.0)**	**307.9 (183.5–371.8)**
Mg^{2+} (mg/L)	19.2	24.2 (18.0–48.5)	**18.7 (18.0–19.8)**	**37.8 (19.9–48.5)**	21.4	29.3 (18.4–52.1)	**21.2 (18.4–23.0)**	**43.2 (28.3–52.1)**
K^+ (mg/L)	2	2.0 (1.3–2.4)	2.1 (1.9–2.4)	1.7 (1.3–2.1)	1.5	1.7 (1.5–2.1)	**1.6 (1.5–2.1)**	**1.9 (1.8–2.1)**
Na^+ (mg/L)	18.1	17.2 (11.9–19.0)	**18.5 (18.0–19.0)**	**13.8 (11.9–17.4)**	22.4	18.5 (9.0–22.5)	**21.5 (19.1–22.5)**	**13.4 (9.0–17.2)**
SO_4^{2-} (mg/L)	74.7	235.1 (71.8–906.1)	**77.6 (71.8–95.3)**	**629.0 (199.2–906.1)**	87.4	319.8 (77.5–924.8)	**88.1 (77.6–122.5)**	**716.9 (324.6–924.8)**
NO_3^- (mg/L)	2.2	1.5 (0.1–3.8)	1.8 (0.1–3.8)	0.8 (0.4–1.3)	2.1	1.2 (0.0–2.4)	**1.6 (0.3–2.4)**	**0.3 (0.1–0.6)**
Cl^- (mg/L)	30.1	28.4 (19.2–31.3)	**30.5 (29.8–31.3)**	**23.2 (19.2–29.6)**	33.8	28.5 (13.6–34.3)	**32.8 (29.2–34.3)**	**21.2 (13.6–27.6)**
F^- (mg/L)	0.1	0.2 (0.1–0.4)	**0.1 (0.1–0.2)**	**0.3 (0.2–0.4)**	0.2	0.2 (0.1–0.4)	**0.1 (0.1–0.2)**	**0.3 (0.2–0.4)**
HCO_3^- (mg/L)	234.3	259.8 (230.2–308.2)	**250.4 (230.2–268.1)**	**289.4 (257.3–308.2)**	270	259.8 (201.8–307.4)	268.4 (256.9–290.2)	244.9 (201.8–307.4)
DO (mg/L)	12.1	3.7 (0.8–9.1)	4.3 (1.6–9.1)	2.1 (0.8–4.6)	9.2	3.1 (0.5–8.5)	4.4 (0.5–8.5)	0.7 (0.6–1.1)
DO (% sat)	137.7 (134.2–139.1)	41.0 (39.4–42.3)	45.7 (45.3–46.2)	21.1 (20.8–21.4)	101.9 (100.2–103.0)	32.9 (32.1–33.3)	–	–
Specific conductance (µS/cm)	541	853 (580–1945)	**599 (580–629)**	**1490 (805–1945)**		1043 (652–1979)	**683 (652–746)**	**1660 (855–1979)**
Temperature (°C)	21.4 (20.8–21.9)	20.0 (18.0–21.6)	**18.0 (17.6–18.5)**	**17.5 (16.7–18.2)**		17.9 (16.7–18.5)	–	–

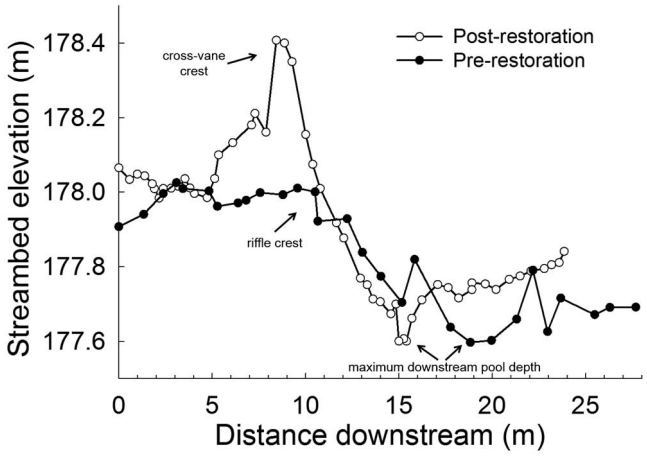

Figure 2. Cross-section of streambed topography along the thalweg pre- and postrestoration.

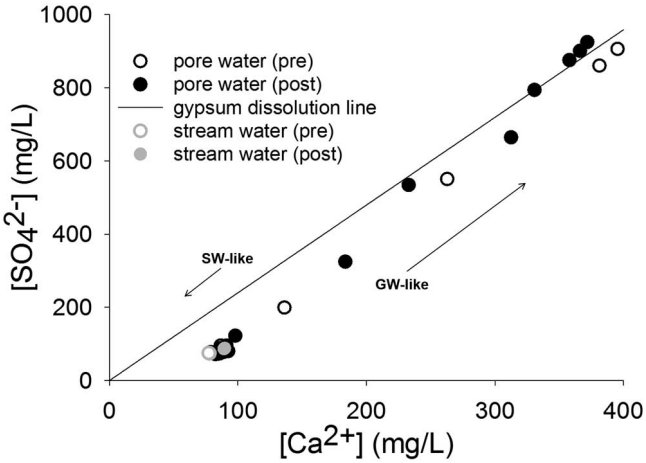

Figure 3. $[SO_4^{2-}]$ vs $[Ca^{2+}]$ in pre- and postrestoration stream and porewater samples and the gypsum dissolution line. Sites with $[Ca^{2+}]$ and $[SO_4^{2-}]$ >120 mg/L and 200 mg/L, respectively, are considered groundwater (GW)-like, and sites with $[Ca^{2+}]$ and $[SO_4^{2-}]$ <120 mg/L and 200 mg/L, respectively, are surface-water (SW)-like.

gradient remained the same (0.02 m/m), but the elevation profile in the reach was much more complex after than before restoration (Fig. 2). Before restoration, the elevation change across the reach occurred primarily near the riffle, whereas after restoration, the elevation change occurred near the cross-vane and engineered rock-riffle (Fig. 2). The engineered rock-riffle was installed where a plunge pool typically would have been excavated (Rosgen 2011), but a natural pool present downstream of the rock-riffle produced streambed elevations as low as those observed before restoration (Fig. 2). Before restoration, the streambed slope was 5% between the crest of the riffle and the bottom of the downstream pool. After restoration the streambed had a 12% slope across the restoration structure from the highest elevation at the cross-vane to the lowest elevation in the downstream pool. The free surface profile was more variable across the cross-vane and engineered rock-riffle than across the prerestoration riffle because of the focused flow toward the stream channel center induced by the cross-vane and the increased slope across the engineered rock-riffle.

Baseflow geochemistry and vertical exchange rates

Prerestoration. During baseflow conditions, SW chemistry was dominated by SO_4^{2-} and Ca^{2+} because of gypsum dissolution from the local bedrock (Table 1, Fig. 3). Surface water had high [DO] and $[NO_3^-]$ and low $[HCO_3^-]$ relative to pore water ($p < 0.01$). Surface-water chemistry was uniform across the stream reach, confirmed by water samples taken at the head and tail of the study reach.

Porewater chemistry also was dominated by gypsum dissolution (Table 1, Fig. 3). Based on the distribution of porewater solute chemistry, streambed sites could be divided into 2 categories: surface-water (SW)-like and groundwater (GW)-like (Fig. 3; Zimmer and Lautz 2014). Zimmer and Lautz (2014) used principal components analysis to interpret variance in prerestoration porewater and SW chemistry at the field site and found that $[SO_4^{2-}]$ and $[Ca^{2+}]$ in pore water primarily reflected the influence of ground water. GW-like sites have $[SO_4^{2-}]$ > 200 mg/L and $[Ca^{2+}]$ > 120 mg/L (Fig. 3). Before restoration, GW-like sites were near the head of the riffle and on the outside of the meander (sites P01, P02, P05, and P09; Figs 1A, 4A, C, E) and had high SC, $[SO_4^{2-}]$, $[Ca^{2+}]$, and $[Mg^{2+}]$ and low [Na^+], $[Cl^-]$, [DO], and $[NO_3^-]$, relative to other sites (Table 1, Figs 1A, 4A, C, E, 5). [DO] ranged from 0.8 to 4.6 mg/L in the GW-like sites and from 1.6 to 9.1 mg/L in the other sites. GW-like sites had upwelling water in the stream bed (Fig. 6A) with an average vertical flux rate of −16 cm/d at the streambed interface (i.e., average of rates seen at the 2.5 and 5.0 cm depths).

SW-like sites had low $[SO_4^{2-}]$, $[Ca^{2+}]$, $[F^-]$, $[HCO_3^-]$, SC, and $[Mg^{2+}]$ and high $[Na^+]$ and $[Cl^-]$ relative to GW-like sites ($p < 0.01$; Table 1, Fig. 4A, C, E). Porewater geochemistry outside of zones affected by GW discharge showed spatial organization of some solutes around the riffle. Mean concentrations of most major cations (Mg^{2+}, Ca^{2+}, Na^+), major anions (HCO_3^-, Cl^-, F^-, SO_4^{2-}), and SC did not differ between SW-like sites within (n = 5; P04, P06, P07, P08, P10) and downstream (n = 4; P11, P12, P13, P14) of the riffle (heteroscedastic 2-tailed Student's t-test, $p > 0.10$). $[NO_3^-]$, $[K^+]$, pH, and [DO] differed between sites within and below the riffle ($p < 0.10$). $[NO_3^-]$ was higher at the riffle sites and $[K^+]$ was higher at the downstream sites (Fig. 4C). Heat-tracing results indicated water downwelling into the stream bed within the riffle with an average vertical flux rate of 8.9 cm/d across the streambed interface and water upwelling downstream of the riffle with an aver-

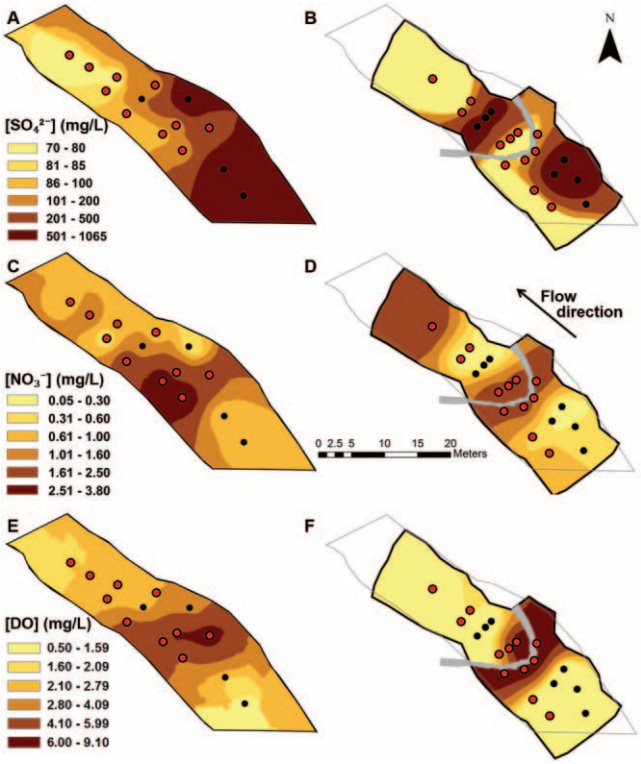

Figure 4. Plan-view maps of pre- (A, C, E) and postrestoration (B, D, F) porewater [SO_4^{2-}] (A, B), [NO_3^-] (C, D), and dissolved O_2 (DO) (E, F) prerestoration during baseflow conditions at 15 cm depth in stream bed. Red circles represent surface-water (SW)-like porewater sites, and black circles represent groundwater (GW)-like porewater sites. See Fig. 1 for explanation of maps.

age vertical flux rate of −15 cm/d (Fig. 6A).Vertical flux rates became neutral or slightly downwelling for all sites below 10 cm (Fig. 7A).

Postrestoration. During baseflow conditions, surface-water and porewater concentrations of solutes were similar before and after restoration, although solute concentrations were slightly higher (except K^+, NO_3^-, DO concentration and % saturation) after restoration (Table 1, Fig. 4B, D, F). After restoration, SW chemistry was dominated by SO_4^{2-} and Ca^{2+} and had higher [Na^+], [NO_3^-], [Cl^-], [HCO_3^-], and [DO] than pore water ($p < 0.002$; Table 1). Surface-water chemistry remained uniform across the reach, confirmed by water samples taken at the head and tail of the reach.

Porewater geochemistry was dominated by gypsum dissolution and the ranges of solute concentrations observed in the hyporheic zone after restoration were similar to those observed before restoration (Table 1, Fig. 4B, D, F). Distinctions between SW-like and GW-like sites were similar before and after restoration. For instance, zones of GW discharge, identified by geochemistry, remained prominent in the upper portion of the study reach, though increased in spatial extent downstream of the cross-vane (sites PA, PC, PD, PE, PN, PO, and PP; Fig. 4B). The zones of GW discharge had higher [SO_4^{2-}], [Ca^{2+}], [K^+], [F^-], and [Mg^{2+}] and lower [NO_3^-], [Na^+], and [Cl^-] than other sites ($p < 0.01$; Table 1, Fig. 4B, D). These GW-like sites had SC values ranging from 855 to 1979 µS/cm, whereas the rest of the streambed sites had SC values from 652 to 746 µS/cm. [DO] ranged from 0.6 to 1.1 mg/L in the GW-like sites and from 0.5 to 8.5 mg/L in the SW-like sites (Table 1). Porewater geochemistry showed spatial organization around the cross-vane and rock-riffle (Fig. 4B, D, F). For instance, [NO_3^-] was low upstream of the cross-vane and in GW-discharge zones, but high adjacent to the cross-vane, in the rock-riffle, and in the upstream section of the next riffle. Geochemistry suggested that GW-influence had expanded downstream of the cross-vane (Fig. 4B), but heat-tracing results were less conclusive because temperature profile rods did not cover the same spatial extent as mini-piezometers (Fig. 1B).

Downwelling increased substantially after restoration. The highest average flux rate at the streambed interface before restoration was 15 cm/d, whereas the highest average flux rate after restoration was 290 cm/d (Figs 6A, B, 7A, B). Within the rock-riffle, downwelling was stronger in the top 10 cm of the stream bed than at depth. At depth, flux rates in the rock-riffle became neutral or slightly downwelling, except for one site that showed slight upwelling (Fig. 6B).

Percent surface water in stream bed: postrestoration

We used a 24-h constant-rate injection of RWT to calculate % surface water in the pore water postrestoration. The concentration of RWT in surface water during plateau varied across the study reach by 2.24 µg/L because of uneven mixing. Thus, % surface water at each

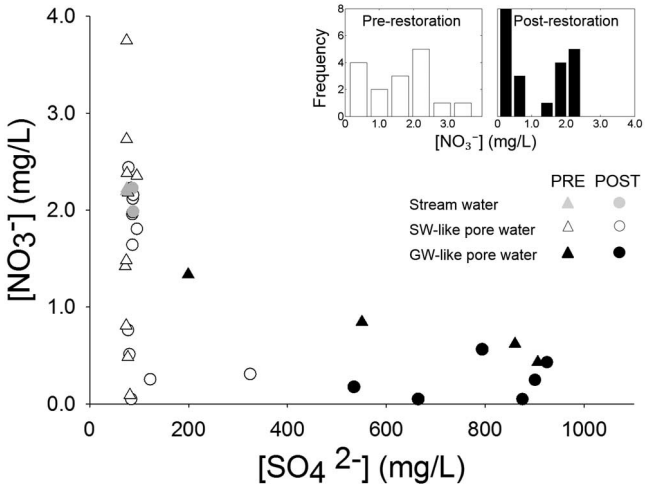

Figure 5. [NO_3^-] vs [SO_4^{2-}] in pre- and postrestoration stream and porewater samples. Insets show pre- and postrestoration histograms for [NO_3^-].

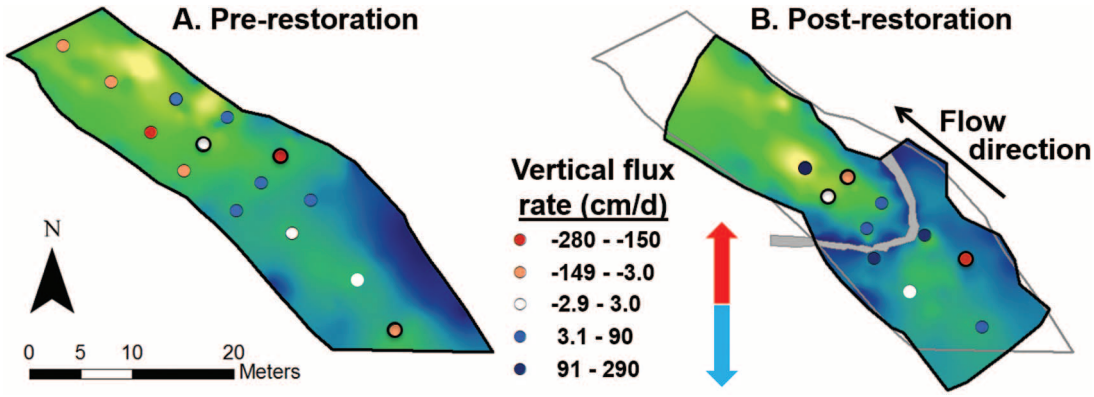

Figure 6. Vertical exchange flux across the streambed interface (average value of fluxes at 2.5 and 5.0 cm depths) during baseflow conditions pre- (A) and postrestoration (B). Red indicates upwelling (negative values) and blue indicates downwelling (positive values). Sites in groundwater discharge zones are indicated by black circles around points. Prerestoration sites in white represent exchange rates that are neutral (close to 0) and postrestoration sites in white represent missing data. See Fig. 1 for an explanation of maps.

piezometer had an uncertainty of 7 to 12%. Pore water at sites near the cross-vane and in the rock-riffle was ~100% surface water, whereas pore water at most other sites consisted of ~20% surface water (Fig. 8). Sites with high surface-water advection were near the cross-vane (Fig. 8). Site PM was in the engineered rock-riffle, but had lower % surface water (~30%) and lower [DO] than other rock-riffle sites. PQ was at the tail of the engineered rock-riffle, but had higher % surface water (~60%), [Cl^-], and [DO] than adjacent sites. PF was in the pool above the cross-vane and had higher % surface water (~35%), higher [Cl^-], and lower [SO_4^{2-}] than nearby sites.

DISCUSSION

Zones of upwelling and downwelling pre- and postrestoration

Restoration produced downward exchange rates adjacent to the cross-vane that were an order of magnitude larger than before restoration (Figs 6A, B, 7A, B). The downwelling was the result of increased spatial heterogeneity along the stream bed, which causes more variability in hydraulic head across the channel, and can cause changes in streambed permeability. In contrast, exchange rates at sites >1 m from the cross-vane and riffle bedform were similar before and after restoration. The geochemistry confirmed the heat-tracing results. Before restoration, the zone of lower [SO_4^{2-}], suggestive of less GW and more SW input, was focused around the inner edge of the meander within and downstream of the riffle (Fig. 4A). After restoration, the zone of lower [SO_4^{2-}] was more prominent adjacent to the cross-vane (Fig. 4B).

Our finding that exchange rates increase near structure is not unique. Daniluk et al. (2013) and Gordon et al. (2013) used methods similar to ours to calculate vertical exchange rates (the VFLUX method) at reference and restored reaches in predominantly agricultural watersheds

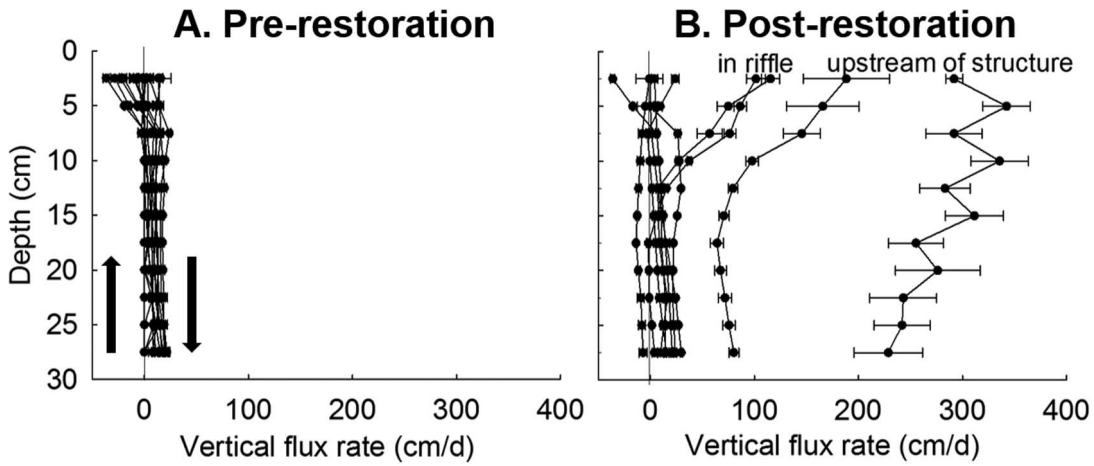

Figure 7. Mean (±1 SD from the calculated mean exchange rate) vertical exchange flux (cm/d) across all depths in the stream bed during baseflow conditions pre- (A) and postrestoration (B).

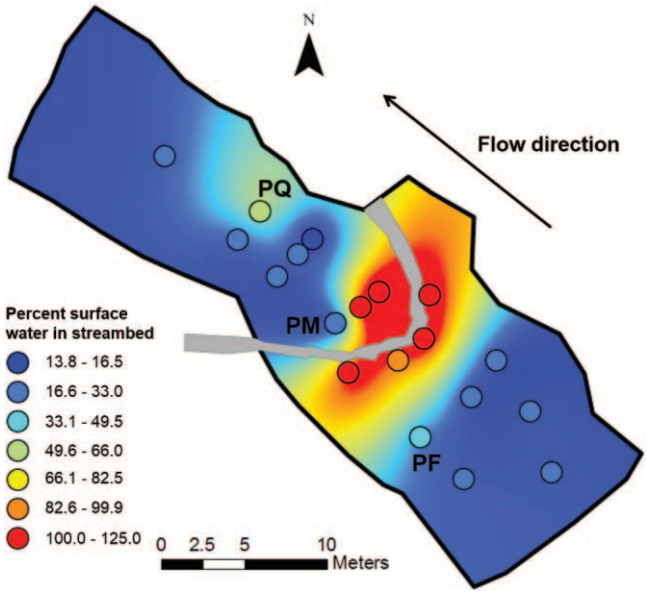

Figure 8. Plan-view map of % surface water (SW) in stream bed during baseflow conditions postrestoration. Contours were interpolated using ArcGIS.

in central New York where the goal of the restoration was to reduce erosion and channel migration. In both studies, upwelling or downwelling at the bed interface was minimal (<40 cm/d) at reference reaches or areas distant from restoration structures, and downwelling into the stream bed was strong (50–350 cm/d) adjacent to restoration structures. In a study of large woody debris, which is analogous to restoration structures, hyporheic exchange rates were affected only at sites ≤2 m from the logs (Sawyer et al. 2012).

Geochemical analyses and heat tracing showed that groundwater upwelling was prominent before and after restoration of our study reach (Figs 4A–F, 6A, B). However, the spatial resolution afforded by heat tracing was too coarse for us to assess changes in the spatial extent of groundwater upwelling after restoration. Porewater geochemistry indicated strong upwelling in the pool above the unrestored riffle and the cross-vane (Fig. 6A, B). However, only 2 mini-piezometers were installed in the upstream pool before the restoration, so we are unable to draw conclusions regarding changes in the extent of groundwater upwelling in that region after restoration (Fig. 4A, B). On the other hand, the zone of groundwater upwelling across the tail of the unrestored riffle bedform appears to have expanded after restoration. Piezometers spanned the width of the stream bed in this area before and after restoration. Groundwater upwelling extended partially across the channel before and entirely across the channel after restoration (Fig. 4A, B). The new structure induces head gradients that are superimposed upon the larger-scale pattern of discharge, thereby focusing groundwater discharge around the cross-vane. Local patterns of exchange can strongly influence patterns of groundwater discharge (Wörman et al. 2007, Stonedahl et al. 2013). Thus, the change we observed might have been caused by a new interaction between hyporheic exchange induced by the cross-vane and the larger-scale patterns of groundwater discharge.

An alternative explanation for the change in the spatial pattern of groundwater upwelling is that machinery may have consolidated the original bed materials during construction of the cross-vane. At the same time, addition of the engineered rock-riffle introduced less consolidated, coarser material to the stream bed. This higher permeability material that might still have been free of fines would increase the near-surface exchange flow induced by the cross-vane and rock-riffle and would increase the separation of the exchange flow from groundwater discharge. A distinct layer of higher permeability materials overlaying lower permeability materials could produce an effective anisotropy that favors flow parallel to the layers and hinders flow and mixing perpendicular to the layers (Marion et al. 2008, Sawyer and Cardenas 2009, Marklund and Wörman 2011).

Daniluk et al. (2013) observed stronger influence of groundwater upwelling on porewater geochemistry in reference reaches than in restored reaches, and concluded that restoration did not enhance the groundwater connection to the stream bed. Our results suggest that restoration shifted the groundwater discharge zone and increased its spatial extent. One explanation for the difference in findings is that Daniluk et al. (2013) studied sites 6 to 8 y after restoration, whereas we studied a newly restored site. Clogging of the top layer of channel sediments can occur over time following restoration, thereby reducing hydraulic conductivity of bed sediments and shifting patterns of surface-water–groundwater interaction through time (Kasahara and Hill 2006). Thus, the distribution of groundwater upwelling may change over time as the restoration structure evolves. An alternative explanation is that Daniluk et al. (2013) used a space-for-time substitution and compared restored and reference sites on different stream reaches. Thus, spatial patterns of groundwater upwelling might have been inherently different between sites.

Biogeochemical differences pre- and postrestoration

We used spatial patterns of solutes indicative of GW inputs, such as SO_4^{2-}, to confirm heat-tracing results in regard to the physical upwelling and downwelling of water within the stream bed. We used spatial patterns in nonconservative solutes as indicators of potential differences in biological activity and nutrient processing in the stream bed before and after restoration. Biogeochemistry is difficult to compare directly between pre- and postrestoration studies because stream discharge and surface-water chemistry differed between dates. However, we are able to interpret relative differences.

[DO] were lower in pore water than in stream water. Concentrations changed little in either compartment after restoration, but prerestoration values were slightly higher than postrestoration values in both compartments (Table 1). DO was supersaturated in stream water before restoration, possibly because higher prerestoration temperatures enhanced primary production, and was saturated after restoration (Table 1). [NO_3^-] in stream water changed little after restoration, whereas [NO_3^-] in pore water was more variable before than after restoration. Before restoration, [NO_3^-] was 0.2 to 1.5 mg/L higher in pore water than in stream water at 4 sites (29% of sites), whereas after restoration, [NO_3^-] was 0.3 mg/L higher in pore water than in stream water at only 1 site (5% of sites) (Fig. 5). Residence time of water in the hyporheic zone strongly regulates the net effects of NO_3^- production on porewater chemistry (Zarnetske et al. 2011, Briggs et al. 2014). Thus, the change in porewater [NO_3^-] in our study suggests that postrestoration porewater residence times in the stream bed are too short for NO_3^- to accumulate, or that the rate of NO_3^- production decreased after restoration. Daniluk et al. (2013) and Gordon et al. (2013) also failed to find strong evidence of elevated [NO_3^-] concentrations associated with NO_3^- production in pore water at restored sites.

The distribution of DO and NO_3^- in pore water across the stream bed differed markedly before and after restoration. Before restoration, [NO_3^-] and [DO] differed widely among sites (Figs 4C, E, 5). However, after restoration both constituents were bimodally distributed. [DO] and [NO_3^-] were high around the hydraulic steps (riffle and cross-vane) before and after restoration. However, after restoration, [NO_3^-] in pore water at sites adjacent to the cross-vane were almost identical to [NO_3^-] in stream water, whereas before restoration [NO_3^-] in pore water at riffle sites were similar to or higher than [NO_3^-] in stream water, presumably because of NO_3^- production in the stream bed. After restoration, sites away from the cross-vane had low and almost identical [NO_3^-], whereas before restoration, sites away from the riffle had a spectrum of [NO_3^-] (Fig. 4C, D). These patterns suggest a broad spectrum of net NO_3^- production and uptake across the hyporheic zone before restoration, but only net uptake in the hyporheic zone after restoration. We compared [NO_3^-] and [SO_4^{2-}] in stream and pore water to assess whether these dynamics were caused by in-stream processes or source-water signatures (Fig. 5). Pore water at SW-like sites had [SO_4^{2-}] similar to stream water, a result indicating that GW inputs did not dilute [NO_3^-] and that the DO and NO_3^- dynamics were caused by in-stream processes.

The bimodal distributions of [NO_3^-] and [DO] after restoration suggest that porewater residence time is bimodally distributed. Very short residence times correspond to conservative NO_3^- transport, whereas longer residence times correspond to low DO and net NO_3^- uptake. Results of the postrestoration RWT constant-rate injection showed a bimodal distribution of % surface water in the pore water. Pore water at the sites adjacent to the restoration cross-vane was composed of ~100% surface water, whereas pore water at sites away from the cross-vane was composed of ~20% surface water (Fig. 8).

Ecological implications

Boulton et al. (1998) argued the importance of the hyporheic zone as an ecotone between the stream and ground water and, thus, as a unique habitat for microbes and invertebrates. Streambed organisms provide valuable ecosystem services by transforming and retaining nutrients in the stream bed, increasing porosity by burrowing, and adding C and other nutrients by processing organic matter. Increasing vertical connectivity has been encouraged as a goal in restoration projects (Boulton 2007, Kasahara et al. 2009, Hester and Gooseff 2010). Restoration practitioners typically do not target improvements in vertical connectivity, but structures that produce hydraulic steps (cross-vanes, engineered riffles, log jams) increase hyporheic exchange (Kasahara and Hill 2006, Lautz and Fanelli 2008, Daniluk et al. 2013) and, thus, opportunities for microbial activity and nutrient transformations (Brunke and Gonser 1997).

[SO_4^{2-}] indicated a shift in the zone of groundwater discharge in the stream bed at the tail end of the engineered rock-riffle after restoration (Fig. 4A, B). This shift suggests that construction of the rock-riffle altered groundwater flow paths, diverted existing upwelling groundwater flow paths to different areas, and increased the aerial extent of the groundwater discharge zone. Groundwater discharge zones may be refugia during large-scale disturbances, such as floods, because surface water may not infiltrate as far into the bed at these locations (Dole-Olivier et al. 1997, Baxter and Hauer 2000). However, these zones lack infiltrating surface water to carry DO and nutrients into the stream bed. Thus, they may hinder microbial activity and decrease productivity. Changes in zones of groundwater discharge may be site specific, but information is lacking about the influence of heavy machinery or introduced rock material on streambed hydraulic conductivity and associated patterns of groundwater discharge.

The bimodal distribution of SW-like and GW-like sites has implications for the effect of restoration on stream health. In our study, restoration produced more SW-like sites, but the net effects on biogeochemical processes are less evident. Our results suggest that securing hyporheic health is not as simple as ensuring that restoration goals include increasing the in-stream hydraulic gradient (via step-pools, engineered riffles, etc.) to maxi-

mize downwelling (Hester and Gooseff 2010, 2011). The restoration must create a balance between carrying DO- and nutrient-rich surface water into the stream bed and ensuring sufficiently long residence times for processes, such as nitrification, to create a net change in porewater concentrations. The prerestoration gradient of porewater chemistry became more bimodal after restoration, a change that leads us to question the functionality of structures that induce rapid downwelling. Findlay (1995) explained that biogeochemical reactions in the hyporheic zone are controlled by processing rates and the % surface water cycling through the system. In our study, the rate of processing was too slow or the residence time too short to increase porewater nutrient concentrations in areas with higher % surface water (adjacent to the cross-vane; Fig. 8). On the other hand, DO and NO_3^- were depleted in areas of the stream bed with low % surface water. Thus, in areas not immediately adjacent to the cross-vane, the rate of stream interaction with the stream bed was uniformly low and porewater chemistry was homogeneous. Thus, our results show that installation of cross-vanes and engineered rock-riffles may limit NO_3^- production across the restored stream reach and eliminate spatial heterogeneity of available DO and nutrients in the stream bed.

Seepage fluxes upstream of a small engineered log dam in Red Canyon Creek, Wyoming, were between 6.6 and 93.6 cm/d (Fanelli and Lautz 2008), almost 200 cm/d slower than flux rates adjacent to the cross-vane in our study. The smaller flux rates above the log jam showed more spatially patchy redox processing in the stream bed, and streambed sites that were SW-like (i.e., no net change in [NO_3^-]) had net NO_3^- production and NO_3^- uptake (Fanelli and Lautz 2008). In our restored reach, patchiness is restricted to sites that are either SW-like or have net NO_3^- uptake, with no real indication of NO_3^- production (Fig. 4D). Crispell and Endreny (2009) show that the size of the restoration structure affects rates of hyporheic exchange. Thus, the cross-vane in our study might have been too large to produce intermediate residence times that permit NO_3^- production to elevate porewater [NO_3^-], as otherwise seen by Fanelli and Lautz (2008).

Gordon et al. (2013) calculated that ~0.4% of stream discharge enters the stream bed in a 50-m reach restored with a cross-vane, and Sawyer et al. (2012) calculated that ~1% of stream discharge interacted with the stream bed around large woody debris in a 5-m flume experiment. Thus, cross-vanes and other stream obstructions increase the rate of vertical exchange of surface water into the stream bed, but the total percentage of surface water that interacts with the stream bed is not large. This low percentage probably is a result of the spatially constrained effect of cross-vanes on vertical connection. Downwelling rates are high at sites immediately adjacent to the cross-vane, but are low at sites >1 m from the cross-vane. Similar results were obtained by Sawyer et al. (2012), who showed that the addition of log structures affected hyporheic exchange only at sites within ~1 to 2 m of the logs. These low volumes of hyporheic exchange around restoration structures indicate low potential for hyporheic exchange to affect surface-water chemistry along restored reaches.

The cross-vane and rock-riffle promoted a bimodal distribution of water flux in the hyporheic zone because rapid downwelling immediately around the cross-vane swamped flux rates elsewhere in the study reach. This bimodal distribution in flux was reflected in the streambed chemistry patterns, which suggested that restoration might not improve stream ecosystem function in the form of biogeochemical processing. Given the high cost of cross-vane installation and the inconclusive improvement of stream-water–groundwater interactions, we suggest exploration of alternative restoration practices designed to improve the vertical connection in stream systems by using more modest hydraulic steps or by using designs that would increase vertical exchange over a spatial extent larger than just immediately adjacent to structures. Furthermore, practitioners should consider the potential negative effects of machinery on streambed permeability.

Conclusion

We examined the spatial response of porewater geochemistry and vertical exchange rates to in-stream restoration across a riffle bedform. We paired baseflow porewater geochemical analyses with calculations of vertical flux rates from heat tracing to compare pre- and postrestoration conditions. The restored site had a steeper slope across the cross-vane and engineered rock-riffle. This hydraulic step enhanced downward vertical flux rates adjacent to the cross-vane by an order of magnitude. These hot spots of vertical exchange introduced solutes and DO into the stream bed, as shown by SW-like porewater solute concentrations. However, the greater vertical flux rates decreased the residence time of water in the subsurface, which minimized the net effects of nutrient processing and promoted a bimodal distribution of geochemistry, % surface water in pore water, and vertical flux rates. Installation of cross-vanes can result in uniform, high-magnitude downwelling of surface water into the hyporheic zone, potentially decreasing diversity of streambed biogeochemical processing.

Groundwater discharge had a greater zone of influence around the tail end of the rock-riffle after restoration. The larger zone of upwelling is hypothesized to be from a change in streambed permeability subsequent to

addition of a higher permeability sediment layer, which increased effective anisotropy and created flow paths parallel to the contact between the new high-permeability layer and the old, lower-permeability layer. Our results suggest that restoration enhanced the streambed connection with surface water and with ground water, but whether the restoration improved the functionality of the hyporheic zone remains questionable. A need exists for future studies to monitor how restoration structures change over time.

ACKNOWLEDGEMENTS

This material is based upon work supported by the National Science Foundation under Grant No. EAR-0911612 and the Syracuse Center of Excellence, through the Collaborative Activities for Research and Technology Innovation (CARTI) program. We thank Aaron Packman, Audrey Sawyer, Erich Hester, and 1 anonymous referee for helpful feedback and suggestions. We thank Martin Briggs, Benjamin Fisher, AnneMarie Glose, Ryan Gordon, and Sarah Ledford for work in the field.

LITERATURE CITED

Battin, T. J., L. A. Kaplan, J. D. Newbold, and C. M. E. Hansen. 2003. Contributions of microbial biofilms to ecosystem processes in stream mesocosms. Nature 426:439–442.

Baxter, C. V., and F. R. Hauer. 2000. Geomorphology, hyporheic exchange, and selection of spawning habitat by bull trout (*Salvelinus confluentus*). Canadian Journal of Fisheries and Aquatic Sciences 57:1470–1481.

Becker, J. F., T. A. Endreny, and J. D. Robinson. 2013. Natural channel design impacts on reach-scale transient storage. Ecological Engineering 57:380–392.

Benson, B. B., and D. Krause. 1980. The concentration and isotopic fractionation of gases dissolved in freshwater in equilibrium with the atmosphere. 1. Oxygen. Limnology and Oceanography 25:662–671.

Benson, B. B., and D. Krause. 1984. The concentration and isotopic fractionation of oxygen dissolved in freshwater and seawater in equilibrium with the atmosphere. Limnology and Oceanography 29:620–632.

Bernhardt, E. S., M. A. Palmer, J. D. Allan, G. Alexander, K. Barnas, S. Brooks, J. Carr, S. Clayton, C. Dahm, J. Follstad-Shah, D. Galat, S. Gloss, P. Goodwin, D. Hart, B. Hassett, R. Jenkinson, S. Katz, G. M. Kondolf, P. S. Lake, R. Lave, J. L. Meyer, T. K. O'Donnell, L. Pagano, B. Powell, and E. Sudduth. 2005. Synthesizing US river restoration efforts. Science 308:636–637.

Boano, F., C. Camporeale, R. Revelli, and L. Ridolfi. 2006. Sinuosity-driven hyporheic exchange in meandering rivers. Geophysical Research Letters 33:L18406.

Boulton, A. J. 2007. Hyporheic rehabilitation in rivers: restoring vertical connectivity. Freshwater Biology 52:632–650.

Boulton, A. J., S. Findlay, P. Marmonier, E. H. Stanley, and H. M. Valett. 1998. The functional significance of the hyporheic zone in streams and rivers. Annual Review of Ecology and Systematics 29:59–81.

Briggs, M. A., L. K. Lautz, and D. K. Hare. 2014. Residence time control on hot moments of net nitrate production and uptake in the hyporheic zone. Hydrological Processes 28: 3741–3751.

Brunke, M. 1999. Colmation and depth filtration within streambeds: retention of particles in hyporheic interstices. International Review of Hydrobiology 84:99–117.

Brunke, M., and T. Gonser. 1997. The ecological significance of exchange processes between rivers and groundwater. Freshwater Biology 37:1–33.

Cardenas, M. B., and J. L. Wilson. 2007. Dunes, turbulent eddies, and interfacial exchange with permeable sediments. Water Resources Research 43. doi:10.1029/2008WR007442

Cardenas, M. B., J. L. Wilson, and V. A. Zlotnik. 2004. Impacts of heterogeneity, bed forms, and stream curvature on subchannel hyporheic exchange. Water Resources Research 40: W08307.

Crispell, J. K., and T. A. Endreny. 2009. Hyporheic exchange flow around constructed in-channel structures and implications for restoration design. Hydrological Processes 23:1158–1168.

Daniluk, T. L., L. K. Lautz, R. P. Gordon, and T. A. Endreny. 2013. Surface water–groundwater interaction at restored streams and associated reference reaches. Hydrological Processes 27:3730–3746.

Dole-Olivier, M.-J., P. Marmonier, and J. L. Beffy. 1997. Response of invertebrates to lotic disturbance: is the hyporheic zone a patchy refugium? Freshwater Biology 37:257–276.

Edler, C., and W. K. Dodds. 1992. Characterization of a groundwater community dominated by *Caecidotea tridentata* (Isopoda). Pages 91–99 *in* J. A. Stanford and J. J. Simons (editors). Proceedings of the 1st International Conference on Ground Water Ecology. American Water Resources Association, Bethesda, Maryland.

Elliott, A. H., and N. H. Brooks. 1997. Transfer of non-sorbing solutes to a streambed with bed forms: theory. Water Resources Research 33:123–136.

Fanelli, R. M., and L. K. Lautz. 2008. Patterns of water, heat, and solute flux through streambeds around small dams. Ground Water 46:671–687.

Findlay, S. 1995. Importance of surface-subsurface exchange in stream ecosystems: the hyporheic zone. Limnology and Oceanography 40:159–164.

Gandy, C. J., J. W. N., and A. P. Jarvis. 2007. Attenuation of mining-derived pollutants in the hyporheic zone: a review. Science of the Total Environment 373:435–446.

Gibert, J., M.-J. Dole-Olivier, P. Marmonier, and P. Vervier. 1990. Surface water–groundwater ecotones. Pages 199– 226 *in* R. J. Naiman and H. Décamps (editors). The ecology and management of aquatic–terrestrial ecotones. United Nations Educational, Scientific, and Cultural Organization, Paris and Parthenon Publishers, Carnforth, UK.

Gibert, J., J. A. Stanford, M.-J. Dole-Olivier, and J. V. Ward. 1994. Basic attributes of groundwater ecosystems and prospects for research. Pages 7–40 *in* J. Gibert, D. L. Danielopol, and J. A. Stanford (editors). Groundwater ecology. Academic Press, San Diego, California.

Gordon, R. P., L. K. Lautz, M. A. Briggs, and J. M. McKenzie. 2012. Automated calculation of vertical pore-water flux from

field temperature time series using the VFLUX method and computer program. Journal of Hydrology 420/421:142–158.

Gordon, R. P., L. K. Lautz, and T. L. Daniluk. 2013. Spatial patterns of hyporheic exchange and biogeochemical cycling around cross-vane restoration structures: the role of the hyporheic zone and implications for stream restoration design. Water Resources Research 49:2040–2055.

Haack, S. K., and B. B. Bekins. 2000. Microbial populations in contaminant plumes. Hydrogeology Journal 8:63–76.

Hakenkamp, C. C., A. Morin, and D. L. Strayer. 2002. The functional importance of freshwater meiofauna. Pages 321–335 *in* S. D. Rundle, A. L. Robertson, and J. M. Schmid-Araya (editors). Freshwater meiofauna: biology and ecology. Backhuys, Leiden, The Netherlands.

Hancock, P. J. 2002. Human impacts on the stream–groundwater exchange zone. Environmental Management 29:761–781.

Hancock, P. J., A. J. Boulton, and W. F. Humphreys. 2005. The aquifer and its hyporheic zone: ecological aspects of hydrogeology. Hydrogeological Journal 13:98–111.

Harvey, J. W., and K. E. Bencala. 1993. The effect of streambed topography on surface-subsurface water exchange in mountain catchments. Water Resources Research 29:89–98.

Hatch, C. E., A. T. Fisher, J. S. Revenaugh, K. Constantz, and C. Ruehl. 2006. Quantifying surface water–groundwater interactions using time series analysis of streambed thermal records: method development. Water Resources Research 42: W10410.

Hayashi, M., and D. O. Rosenberry. 2002. Effects of ground water exchange on the hydrology and ecology of surface water. Ground Water 40:309–316.

Hendricks, S. P. 1996. Bacterial biomass, activity, and production within the hyporheic zone of a north-temperate stream. Archiv für Hydrobiologie 136:467–487.

Hester, E. T., and M. W. Doyle. 2008. In-stream geomorphic structures as drivers of hyporheic exchange. Water Resources Research 44:W03417.

Hester, E. T., and M. N. Gooseff. 2010. Moving beyond the banks: hyporheic restoration is fundamental to restoring ecological services and functions of streams. Environmental Science and Technology 44:1521–1526.

Hester, E. T., and M. N. Gooseff. 2011. Hyporheic restoration in streams and rivers. Pages 167–187 *in* A. Simon, S. J. Bennett, and J. M. Castro (editors). Stream restoration in dynamic fluvial systems: scientific approaches, analyses, and tools. American Geophysical Union, Washington, DC.

Hey, R. D. 2006. Fluvial geomorphological methodology for natural stable channel design. Journal of the American Water Resources Association 42:357–374.

Kasahara, T., T. Datry, M. Mutz, and A. J. Boulton. 2009. Treating causes not symptoms: restoration of surface–groundwater interactions in rivers. Marine and Freshwater Research 60:976–981.

Kasahara, T., and A. R. Hill. 2006. Effects of riffle-step restoration on hyporheic chemistry in N-rich lowland streams. Canadian Journal of Fisheries and Aquatic Sciences 63:120–133.

Kilpatrick, F. A., and E. D. Cobb. 1985. Measurement of discharge using tracers. Chapter A16 *in* Techniques of Water-Resources Investigations. Book 3. US Geological Survey, Reston, Virginia.

Knust, A. E., and J. J. Warwick. 2009. Using a fluctuating tracer to estimate hyporheic exchange in restored and unrestored reaches of the Truckee River, Nevada, USA. Hydrological Processes 23:1119–1130.

Lautz, L. K., and R. M. Fanelli. 2008. Seasonal biogeochemical hotspots in the streambed around restoration structures. Biogeochemistry 91:85–104.

Lave, R. 2009. The controversy over natural channel design: substantive explanations and potential avenues for resolution. Journal of American Water Resources Association 45: 1519–1532.

Marion, A., A. I. Packman, M. Zaramella, and A. Bottacin-Busolin. 2008. Hyporheic flows in stratified beds. Water Resources Research 44:W09433.

Marklund, L., and A. Wörman. 2011. The use of spectral analysis-based exact solutions to characterize topography-controlled groundwater flow. Hydrogeological Journal 19:1531–1543.

Marmonier, P., P. Vervier, J. Gibert, and M.-J. Dole-Olivier. 1993. Biodiversity in ground waters. Trends in Ecology and Evolution 8:392–395.

Morrice, J. A., H. M. Valett, C. N. Dahm, and M. E. Campana. 1998. Alluvial characteristics, groundwater-surface water exchange and hydrological retention in headwater streams. Hydrological Processes 11:253–267.

Nogaro, G., T. Datry, F. Mermillod-Blondin, S. Descloux, and B. Montuelle. 2010. Influence of streambed sediment clogging on microbial processes in the hyporheic zone. Freshwater Biology 55:1288–1302.

Rosgen, D. L. 1994. A classification of natural rivers. Catena 22: 169–199.

Rosgen, D. L. 1998. The reference reach: a blueprint for natural channel design. Pages 1009–1016 *in* D. F. Hays (editor). Proceedings of ASCE Specialty Conference on Restoration, American Society of Civil Engineers, Denver, Colorado.

Rosgen, D. L. 2001. Cross-vane, w-weir, and j-hook vane structures: description, design and application for stream stabilization and river restoration. Pages 1–22 *in* D. F. Hays (editor). Proceedings of the Wetlands Engineering and River Restoration Conference. American Society of Civil Engineers, Reno, Nevada.

Rosgen, D. L. 2011. Natural channel design: fundamental concepts, assumptions, and methods. Pages 69–95 *in* A. Simon, S. J. Bennett, and J. M. Castro (editors). Stream restoration in dynamic fluvial systems: scientific approaches, analyses, and tools. American Geophysical Union, Washington, DC.

Sawyer, A. H., and M. B. Cardenas. 2009. Hyporheic flow and residence time distributions in heterogeneous cross-bedded sediment. Water Resources Research 45:W08406.

Sawyer, A. H., M. B. Cardenas, and J. Buttles. 2012. Hyporheic temperature dynamics and heat exchange near channel-spanning logs. Water Resources Research 48:W01529.

Schälchli, U. 1992. The clogging of coarse gravel river beds by fine sediment. Hydrobiologia 235:189–197.

Smith, J. J., and P. S. Lake. 1993. The breakdown of buried and surface-placed leaf litter in an upland stream. Hydrobiologia 271:141–148.

Stanford, J. A., and J. V. Ward. 1993. An ecosystem perspective of alluvial rivers: connectivity and the hyporheic corridor. Journal of the North American Benthological Society 12:48–60.

Stonedahl, S. H., J. W. Harvey, J. Detty, A. Aubeneau, and A. I. Packman. 2012. Physical controls and predictability of stream hyporheic flow evaluated with a multi-scale model. Water Resources Research 48:W10513.

Stonedahl, S. H., J. W. Harvey, and A. I. Packman. 2013. Interactions between hyporheic flow produced by stream meanders, bars, and dunes. Water Resources Research 9:5450–5461.

Strayer, D. L. 1994. Limits to biological distributions in groundwater. Pages 287–313 *in* J. Gibert, D. L. Danielopol, and J. A. Stanford (editors). Groundwater ecology. Academic Press, San Diego, California.

Toran, L., B. Hughes, J. Nyquist, and R. Ryan. 2012. Using hydrogeophysics to monitor change in hyporheic flow around stream restoration structures. Environmental and Engineering Geosciences 18:83–97.

Triska, F. J., J. H. Duff, and R. J. Avanzino. 1993. The role of water exchange between a stream and its hyporheic zone in nitrogen cycling at the terrestrial–aquatic interface. Hydrobiologia 251: 167–184.

Vervier, P., J. Gibert, P. Marmonier, and M.-J. Dole-Olivier. 1992. A perspective on the permeability of the surface freshwater-groundwater ecotone. Journal of the North American Benthological Society 11:93–102.

Ward, A. S., M. N. Gooseff, and P. A. Johnson. 2011. How can subsurface modifications to hydraulic conductivity be designed as stream restoration structures? Analysis of Vaux's conceptual models to enhance hyporheic exchange. Water Resources Research 47:W08512.

Wörman, A., A. I. Packman, L. Marklund, J. W. Harvey, and S. H. Stone. 2007. Fractal topography and subsurface water flows from fluvial bedforms to the continental shield. Geophysical Research Letters 34:L07402.

Zarnetske, J. P., R. Haggerty, S. M. Wondzell, and M. A. Baker. 2011. Dynamics of nitrate production and removal as a function of residence time in the hyporheic zone. Journal of Geophysical Research 116:G01025.

Zimmer, M. A., and L. K. Lautz. 2014. Temporal and spatial response of hyporheic zone geochemistry to a storm event. Hydrological Processes 28:2324–2337.